HYDROLOGICAL PROCESSES
Hydrol. Process. **13**, 139–155 (1999)

Tracer and hydrometric study of preferential flow in large undisturbed soil cores from the Georgia Piedmont, USA

Janice McIntosh,[1]* Jeffrey J. McDonnell[1] and Norman E. Peters[2]
[1]*SUNY College of Environmental Science and Forestry, 1 Forestry Dr., Syracuse, NY 13210, USA*
[2]*US Geological Survey, 3039 Amwiler Rd, Suite 130, Atlanta, GA 30360-2824, USA*

Abstract:

We studied the temporal patterns of tracer throughput in the outflow of large (30 cm diameter by 38 cm long) undisturbed cores from the Panola Mountain Research Watershed, Georgia. Tracer breakthrough was affected by soil structure and rainfall intensity. Two rainfall intensities (20 and 40 mm hr^{-1}) for separate Cl^- and Br^- amended solutions were applied to two cores (one extracted from a hillslope soil and one extracted from a residual clay soil on the ridge). For both low and high rainfall intensity experiments, preferential flow occurred in the clay core, but not in the hillslope core. The preferential flow is attributed to well-developed interpedal macrochannels that are commonly found in structured clay soils, characteristic of the ridge site. However, each rainfall intensity exceeded the matrix infiltration capacity at the top of the hillslope core, but did not exceed the matrix infiltration capacity at the middle and bottom of the hillslope core and at all levels in the clay core. Localized zones of saturation created when rainfall intensity exceeds the matrix infiltration capacity may cause water and tracer to overflow from the matrix into macrochannels, where preferential flow occurs to depth in otherwise unsaturated soil. Copyright © 1999 John Wiley & Sons, Ltd.

KEY WORDS macropores; preferential flow; hydrologic pathways; chloride; bromide; soil moisture; time domain reflectometry; breakthrough curve; matric potential

INTRODUCTION

Previous research on two-domain soils has attempted to describe and partition the movement of water and solutes within and between the soil matrix and macropores (Anderson and Bouma, 1977; Rao *et al.*, 1980a; Luxmoore, 1981; Skopp *et al.*, 1981; Chen and Wagenet, 1992). Macrochannels, defined herein as well connected macropores, have been attributed to the preferential vertical movement of soil water and tracer. Previous studies have shown that water movement through these interconnected channels may bypass to depth, rather than move along a more tortuous route through the soil matrix (Bouma and Dekker, 1978; Mosley, 1979; Beven and Germann, 1982; Tsukamoto and Ohta, 1988; Jabro *et al.*, 1994).

Factors affecting preferential flow include: (1) soil structure (Seyfried and Rao, 1987; Chen and Wagenet, 1992; Buttle and Leigh, 1995; Tindall *et al.*, 1995); (2) soil hydraulic properties and profiles (van Stiphout *et al.*, 1987; Jardine *et al.*, 1990; Kung, 1990); and (3) rainfall intensity (Bouma and Dekker, 1978; Bouma,

* Correspondence to: J. McDonnell, SUNY College of Environmental Science and Forestry, 1 Forestry Drive, Syracuse, NY 13210, USA.

Contract grant sponsor: National Science Foundation.
Contract grant number: EAR 9406436.

CCC 0885–6087/99/020139–17$17·50

Received 10 July 1997
Revised 10 March 1998
Accepted 20 March 1998

1981; Trudgill *et al*., 1983; Booltink, 1994). During high intensity rainstorms, the soil matrix infiltration capacity may be quickly exceeded, thereby inducing overflow of soil water from the matrix into interpedal macrochannels. Macrochannels may transmit water and solutes rapidly to depth as long as the flow rate within the macrochannels exceeds the adsorption rate into the surrounding matrix (Bouma *et al*., 1978). Water and solute movement within and between the matrix and macrochannels has been shown to be a function of hydraulic and concentration gradients, but this relationship is not well understood (Jardine *et al*., 1990; Luxmoore *et al*., 1990). The poor understanding of macrochannel flow processes is due to the often black-box nature of subsurface flow, the complexity of the unsaturated flow system and problems associated with research methodologies.

Field studies lack the physical controls needed to examine properly the factors controlling preferential flow (Trudgill *et al*., 1983; Tsuboyama *et al*., 1994). In contrast, laboratory experiments of solute transport often neglect hydrometric analysis. Furthermore, subsequent modelling of the relative contributions to flow from the soil matrix and macrochannels is often based on qualitative analysis of breakthrough curves (BTCs) (Skopp *et al*., 1981; Smettem, 1984). Soil samples used in laboratory experiments are generally too small to comprise an adequate representative elementary volume (Bouma, 1981). Results obtained from laboratory experiments using artificial soil structures (sieved soil, glass beads or artificial aggregates) do not approximate natural structured soils (Rao *et al*., 1980b; Smettem, 1986; Buttle and Leigh, 1995). The research reported herein focuses on vertical preferential movement of water and conservative tracers in large (30 cm diameter by 38 cm long), undisturbed soil cores. This study is part of a larger effort to examine and model the movement of water and solutes at the hillslope scale (Huntington *et al*., 1993; McDonnell *et al*., 1996; Freer *et al*., 1997).

Field rationale for laboratory study

Previous field research at the Panola Mountain Research Watershed (PMRW), 25 km south-east of Atlanta, where soil cores were extracted for this study, suggests that preferential flow influences vertical movement of water and tracers. For example, Huntington *et al*. (1994) applied 46 g m^{-2} lithium bromide to a 20 m × 20 m area on a forested ridgetop site underlain by a 4-m deep regolith. Bromide (Br^-) migration was monitored by analysis of bulk soil solution extracted from soil samples, tension lysimeter water and groundwater (Figure 1). Huntington *et al*. (1994) found that macrochannels were effective preferential pathways in unsaturated conditions in the south-western ridge of PMRW. Huntington *et al*.'s (1994) results were similar to those observed by both Jardine *et al*. (1990), who studied a soil pedon in Walker Branch Watershed, Tennessee, and McDonnell (1990), who studied subsurface hydrological pathways at the Maimai (M8) Catchment, New Zealand. Jardine *et al*. (1990) and McDonnell (1990) suggested that rainfall created localized zones of saturation, which caused water and tracer lateral movement from small to large pores that channelled water and tracer to depth. Huntington *et al*.'s (1994) results, however, were uncertain because of the periodic, non-event based sampling scheme used in that research. Off-site movement of Br^- further complicated the interpretation of results and the computation of Br^- mass transport.

Hydrometric measurements have also been made at the soil core extraction site. N. E. Peters (US Geological Survey, written communication, 1994) measured temporal and spatial variations in soil moisture using TDR and groundwater level measurements at a PMRW ridgetop forested site (adjacent to the LiBr tracer site). An analysis of the hydrometric data suggests that water was transmitted rapidly to depth during moderate to high magnitude rainstorms as well as during smaller magnitude rainstorms in wet periods (Figure 2). The 183 cm deep ridgetop well in Figure 2 is 3 m from the TDR site. The well consists of 5·1 cm diameter PVC screened over the bottom 76 cm and is monitored using a float-counterweight, potentiometer system (Peters, 1994). The downslope well in Figure 2 is located 15 m from the ridgetop well and is 259 cm deep with a screen and monitoring assembly similar to the ridgetop well.*

* The soil at the ridgetop site contains an aquitard at about 185 cm, as evidenced by previous measurements of soil moisture tension throughout the 4 m soil/regolith profile (Art White, US Geological Survey, personal communication, 1995). The aquitard probably does not exist in the soil at the downslope well due to downslope instability and mass wasting.

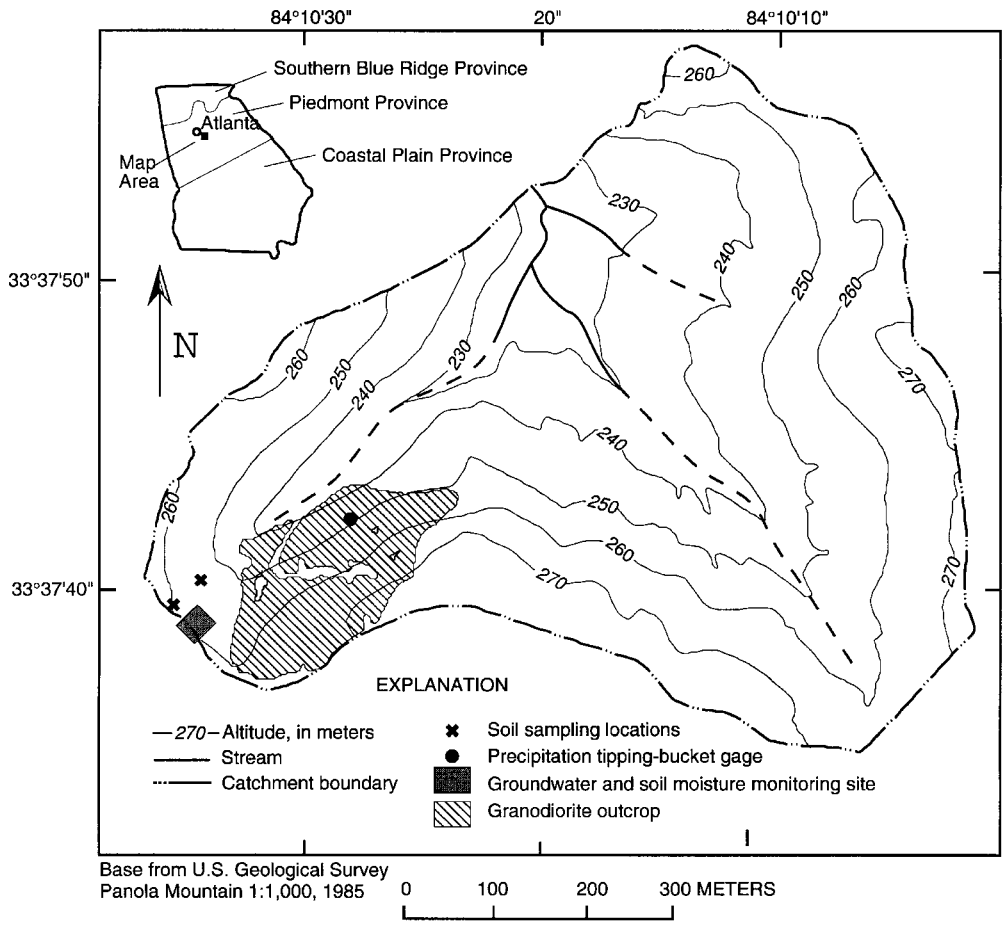

Figure 1. Location of study sites at the Panola Mountain Research Watershed, Georgia

The hydrological response of the ridgetop site to an intermediate intensity, 34 mm rainstorm on 4–5 of April 1993 and a 15 mm rainstorm on 9 April, when the catchment was relatively wet, is shown in Figure 2. Neither TDR volumetric soil moisture contents nor groundwater elevations were calibrated. However, the relative changes and timing of the changes in soil moisture content and groundwater levels relative to rainfall, indicate a rapid change in the surface soil horizon moisture content and a corresponding change in the saturated zone at depth. A change in water content at intermediate soil depths in the unsaturated zone did not occur until after the groundwater response. A wetting front, however, moved uniformly through the unsaturated zone as evidenced by the change in moisture content sequentially at each TDR probe pair with depth through the soil profile. These results, and data for other storms throughout the year, suggest that preferential flow occurs at PMRW, and that the timing of matrix flow is strongly dependent on rainfall intensity and magnitude, and antecedent soil wetness.

The laboratory study reported herein builds upon the studies reported above by using hydrometric and tracer techniques on large (30 cm diameter by 38 cm long), undisturbed soil cores taken from different catchment areas to evaluate: (1) the influence of rainfall intensity on tracer arrival time and breakthrough from the cores; (2) the influence of inferred soil structure on the relative contributions of soil matrix and macrochannel flow to core export; and (3) the influence of rainfall intensity and inferred soil structure on soil saturation.

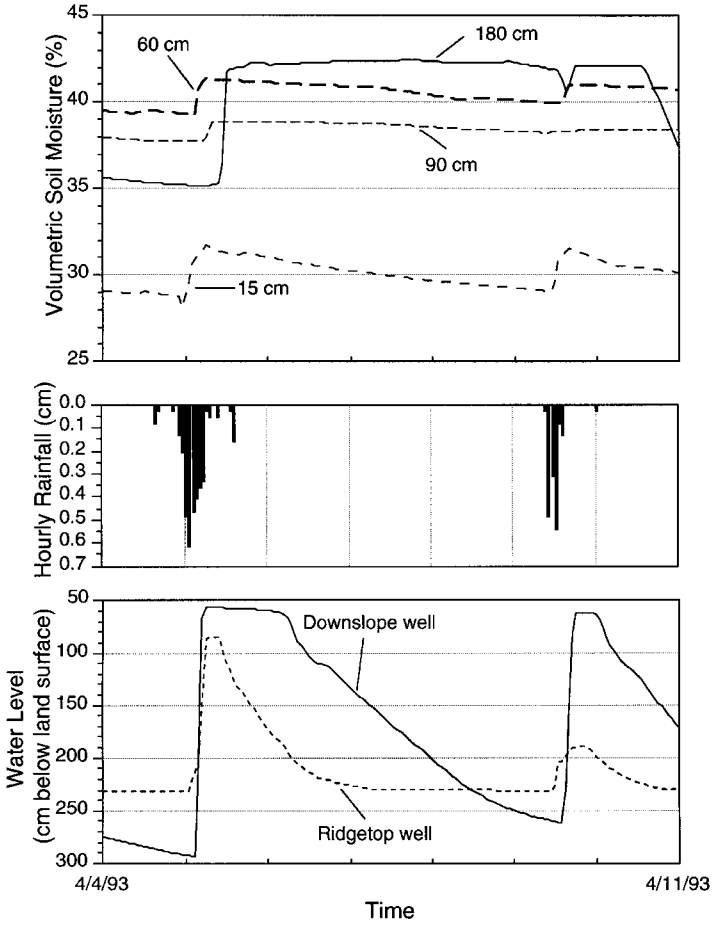

Figure 2. Temporal variations in volumetric soil moisture content of horizontal TDR probes at several soil depths, rainfall rate and groundwater levels at and adjacent to a ridgetop site at the Panola Mountain Research Watershed during 4–11 April 1993

STUDY SITE

PMRW is located about 25 km south-east of Atlanta, Georgia (longitude 84°10′W, latitude 33°37′N). The watershed is 95% forested, dominated by southern hardwood and loblolly pine (Cappellato and Peters, 1995). The watershed is a headwater catchment and the slopes are somewhat steeper than average for the southern Piedmont physiographical province (Huntington *et al.*, 1993). The US Geological Survey (USGS) has monitored a variety of hydrological and biogeochemical parameters in the 41 ha watershed since 1985. For the 1986–1995 water years (October–September), rainfall averaged 1190 mm yr^{-1}, runoff averaged 364 mm yr^{-1} (30% water yield) and air temperature averaged 15 °C.

Soils are mainly Ultisols developed in colluvium and residuum intergrading to Inceptisols in highly eroded landscape positions (Huntington *et al.*, 1993). Entisols occur near stream banks. Soil and saprolite depths are highly variable throughout the catchment, but the regolith averages from 1 to 2 m thick on the hillslopes underlain by the Panola Granite; thicker deposits are located near the stream channels. The Ashlar–Wake complex occurs on the side slopes near the southwestern ridge, where the dominant clay mineral is kaolinite. The Ashlar–Wake complex is described as very bouldery slopes ranging from 15 to 45%.

The south-western watershed ridge soils (Figure 1) are from the Madison series which is characterized by a yellowish brown, sandy loam to 15 cm depth and a strong brown sandy clay loam from 15 to 23 cm. Red clay

is present from 23 to 76 cm, yellowish red sandy clay loam extends from 76 to 89 cm. A yellowish red saprolite, dominated by a mica schist, extends through the remaining profile. Depth to bedrock is typically more than 2 m.

Hillslope soils exist downslope from the ridgetop. These soils are from the Ashlar–Wake complex and are characterized by a very dark, greyish brown sandy loam surface layer to 7 cm depth and a yellowish brown sandy loam subsoil. Material underlying the subsoil is typically a brown, sandy loam to approximately 66 cm, followed by a soft bedrock layer of highly weathered granite to 86 cm and a hard bedrock layer.

METHODS

Large 'undisturbed', intact soil cores (30 cm diameter by 38 cm long) were extracted from two separate PMRW sites using the extraction technique described by Tindall *et al*. (1992). One core was extracted from the south-western ridge and one core was extracted from the soils downslope of the ridge site (Figure 1).* Four small soil cores (5 cm diameter by 30 cm long) were also extracted from each site for laboratory bulk density (D_b) analysis.

The small soil cores were carefully cut at the observed soil horizon boundaries, producing discrete 'horizon' cores of known volume. Each core was then saturated from the base to the top, and placed on a tension table. Tension was applied simultaneously to each core in discrete increments. Cores were allowed to equilibrate and were weighed between applied tension. After all tension had been applied, the cores were oven-dried at 105 °C for 24 hours. D_b values were determined for each horizon core. The experimental D_b values were used to determine large core porosities as follows (Klute and Dirksen, 1986)

$$\text{Porosity} = 1 - (D_b/D_p)$$

where D_b = bulk density (g cm^{-3}) and D_p = particle density, (2·65 g cm^{-3}). The length of observed soil horizons were measured and multiplied by the calculated respective porosity values to determine total large core pore volumes. (see Table III, later).

The south-western ridge soils are clayey, kaolinitic, thermic Kanhapludults from the Madison series. These soils are well drained, moderately permeable and are formed in the residuum weathered from felsic and intermediate, micaceous high-grade metamorphic rock. The hillslope soils are coarse-loamy, mixed, thermic Typic dystrochrepts from the Ashlar series. These are moderately deep and well drained soils formed from the weathered products of granite and gneiss. Soils from the Ashlar series are permeable and drainage is rapid throughout these soils.

Each of the large cores contained many large tree roots to depth but remained intact after extraction at a field laboratory. Once extracted, each core was placed on a 1 bar, high-flow porous ceramic plate, which rested on an aluminum plate and foundation, and was encased in paraffin to preserve soil structure as outlined in Tindall *et al*. (1992). All cores were transported to the SUNY College of Environmental Science and Forestry, Soil Physics Laboratory for subsequent study.

Laboratory preparation and analysis

Carbon dioxide was applied to the base of each core through an inlet tube in the centre of the aluminum plate for 24 hours. Carbon dioxide is more soluble than air, and flushing the core with CO_2 reduces air entrapment. After flushing with CO_2, each core was treated with a deaerated (0·02 M) $Ca(NO_3)_2 \cdot 4H_2O$ solution to minimize colloidal dispersion into the soil solution. Each core was slowly saturated from below for 1–2 days, until a 5 cm head existed on each core.

Three recording tensiometers (McDonnell, 1993) were inserted into each saturated core to measure matric and pressure potential (Figure 3). The tensiometers were inserted into holes of slightly smaller diameter,

* A total of six cores were extracted from the sites — the four cores not discussed in the results section were used as test cores for preliminary analysis of core response and tracer breakthrough.

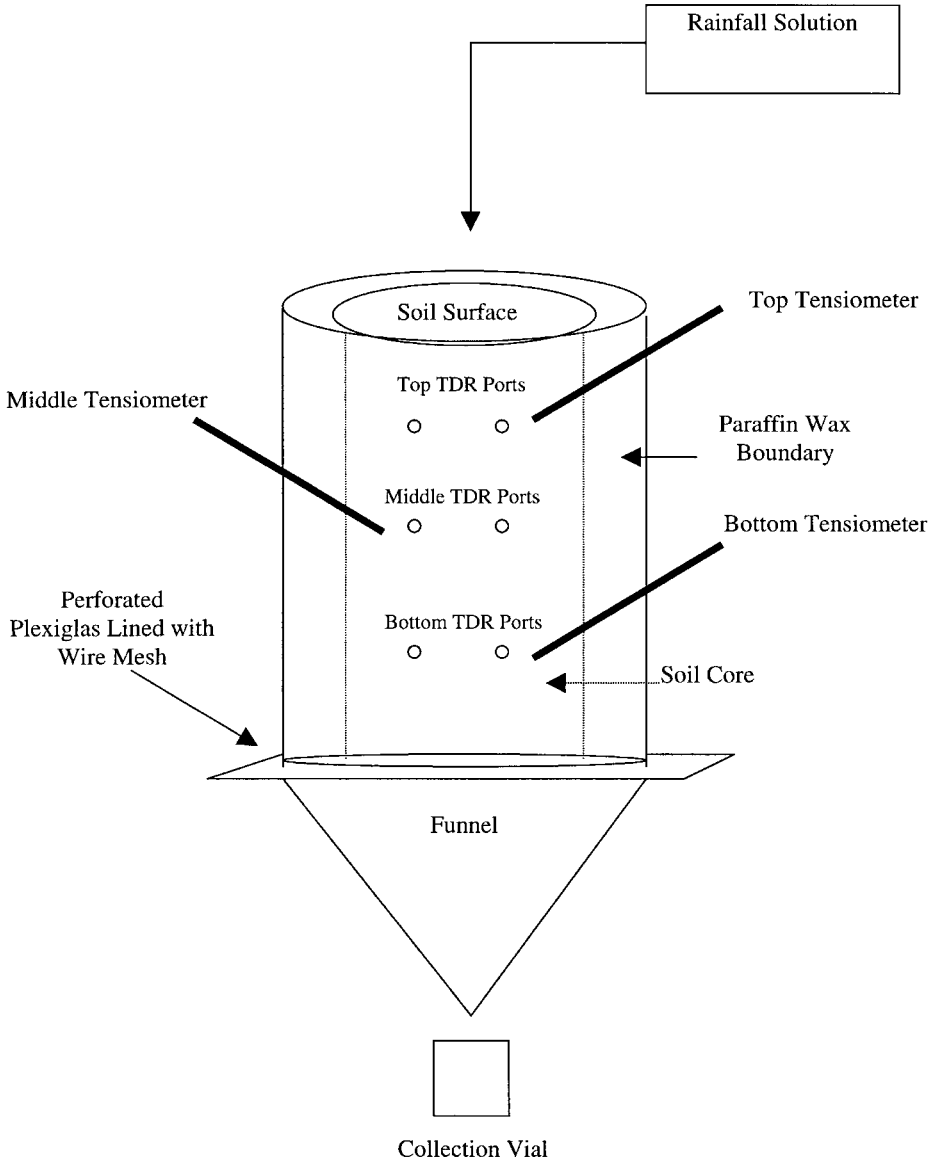

Figure 3. Instrumentation for the soil core experiments

drilled at a 40° angle through the paraffin wax and core. Tensiometer porous cups were positioned in the centre of the core at 10, 20 and 30 cm vertically from the core soil surface. After tensiometer insertion, the paraffin wax boundary was resealed.

In situ soil water characteristic (drainage) curves were obtained by continuous recording of soil moisture tension after disconnecting the inlet tube from the $Ca(NO_3)_2 \cdot 4H_2O$ solution and allowing the core to drain. Twenty-four hours after obtaining the drainage curve, the ceramic and aluminum plates were detached from each core base and replaced with wire mesh-lined, perforated plexiglass. For each core, the plate removal disturbed the lower 5 cm of soil. The disturbed material was removed with a sharp knife. A large PVC funnel (Figure 3) was placed beneath the perforated plexiglass to collect drainage during rainfall simulation experiments.

Before rainfall simulations were conducted and between runs, the hillslope and clay core antecedent moisture conditions were equivalent to each other. Two rainfall simulations, or runs, were completed. The rainfall apparatus consisted of a calibrated, oscillating sprinkler system suspended approximately 30 cm above the core surface. Water was applied to the core surface as evenly as possible during each rainfall simulation. Run 1 consisted of 2 l of (0·025 M) $CaCl_2$ sprinkled on each core at 20 mm hr^{-1}, followed by two pore volumes of tracer-free (0·02 M) $Ca(NO_3)_2 \cdot 4H_2O$. Run 2 consisted of 2 l (0·025 M) $CaBr_2 \cdot 2H_20$ sprinkled on each core at 40 mm hr^{-1}, followed by two pore volumes of tracer-free (0·02 M) $Ca(NO_3)_2 \cdot 4H_2O$. Effluent flow (outflow) from the core base was continuously collected, until drainage ceased, through a funnel positioned underneath the core base that drained into a glass jar. Drainage was transferred at 20 minute intervals from the glass jar into a beaker and measured. At the 20 minute point, a discrete outflow sample was collected by removing the glass jar from the core base and replacing it with a 50 ml collection vial. The vial was analysed for tracer concentration using a Fisher ion selective electrode (precision of ± 5 mg l^{-1}). The discrete samples represented the tracer concentration at that point in time for the experiment.

Model

An approximate analytical model was applied to each rainfall simulation (Rose *et al.*, 1982). For each core, the mean solute penetration depth (about which dispersion occurs) was computed for vertical leaching of non-sorbed solutes by solving the dispersion equation when the mean solute penetration depth was known. The mean solute penetration depth was associated with the maximum solute concentration. In previous studies, the Rose *et al.* (1982) model provided a useful interpretation of experimental data by assuming the convective/dispersion equation was valid under non-steady-state conditions when an equivalent constant flux was used (see Chichester and Smith, 1978).

In this study, the Darcian equivalents for dispersivity (ε) and mobile water content (θ_m) for each core were determined using the simple model efficiency maximization equation, EFF (Buttle and Leigh, 1995):

$$\mathrm{EFF} = \frac{\left[\sum_{i=1}^{n}(O_i - \sigma)^2 - \sum_{i=1}^{n}(O_i - P_i)^2\right]}{\sum_{i=1}^{n}(O_i - \sigma)^2}$$

where O_i is the observed value at time period i, O is the mean of the observed values, P_i is the predicted value at time period i and n is the number of time periods.

Predicted breakthrough curves (BTCs) were obtained by maximizing the model efficiency equation. Owing to the lack of a rigorous optimization technique, ε and θ_m values may not be well defined. Therefore, although these values provide a means of comparison between each core, their physical meaning to PMRW field situations is uncertain (Buttle and Leigh, 1995).

RESULTS

The outflow from each core base, BTCs and internal hydrometric and model results are compared below for the hillslope and clay cores. The results are separated by run. The results of the soil physics characterization are summarized in Table I. A summary of the mass balances for both cores during runs 1 and 2 is provided in Table II.

Outflow hydrographs

Run 1. Core outflow for the hillslope and clay cores is shown in Figure 4A and 4. The mean and range in outflow were similar for each soil during run 1. Hillslope core outflow began 0·13 hr after rainfall

Table I. Soil physics data: bulk density (D_b), porosity, and K_{sat} values obtained from small (5 cm diameter by 30 cm) cores extracted from PMRW study sites. D_b obtained from the gravimetric method, K_{sat} values obtained from the constant head method. Porosity time domain reflectometry (TDR) obtained from *in situ* rod pairs located in the top (10 cm), middle (20 cm), and bottom (30 cm) horizons of the large, experimental cores. K_{un} calculated by the method of Sami and Buttle (1991)

Core position	D_b (g cm^{-3})	$K_{sat\ (cms^{-1})}$	K_{un} (cm s^{-1}) Run 1	K_{un} (cm s^{-1}) Run 2	Porosity (small cores)	Porosity (TDR)	pv (l)
Hillslope core							
Top	NA*	$1{\cdot}79 \times 10^{-2}$	$1{\cdot}19 \times 10^{-4}$	$1{\cdot}98 \times 10^{-4}$	NA	0·65	11·09
Middle	1·41		$7{\cdot}83 \times 10^{-3}$	$8{\cdot}67 \times 10^{-3}$	0·47	0·58	
Bottom	1·38		$1{\cdot}93 \times 10^{-2}$	$1{\cdot}88 \times 10^{-2}$	0·48	0·51	
Clay core							
Top	1·22	$4{\cdot}20 \times 10^{-2}$	$2{\cdot}43 \times 10^{-2}$	$3{\cdot}06 \times 10^{-2}$	0·54	NA	11·03
Middle	1·57		$3{\cdot}36 \times 10^{-2}$	$6{\cdot}08 \times 10^{-2}$	0·42	0·49	
Bottom	1·56		$5{\cdot}60 \times 10^{-2}$	$4{\cdot}58 \times 10^{-2}$	0·41	0·52	

* NA is not available.

Table II. The collected total outflow, measured flux and calculated change in storage from each core base during runs 1 and 2. The calculated % of tracer recovery is presented as a percentage of total applied tracer for each core during runs 1 and 2

	Total outflow (l)	Δ Storage (l)	% Tracer recovered (mg)	Observed flux (mm/hr)
Hillslope core				
Run 1	24·0	+1·4	85	18·8
Run 2	26	−0·3	105	17·6
Clay core				
Run 1	21	+4·5	90	17·6
Run 2	22	+3·5	109	41·4

commenced, ranged from 13 to 21 mm hr^{-1}; and averaged 18·8 mm hr^{-1}. Clay core outflow began 0·38 hr after rainfall commenced, ranged from 11 to 20 mm hr^{-1}; and averaged 17·6 mm hr^{-1}.

For the hillslope core, only one early drainage pulse, which attained a maximum of 16 mm hr^{-1} at 1 hr into run 1, was observed (Figure 4A). Outflow then decreased at 2 hr before increasing to 19 mm hr^{-1} at 3 hr and remained relatively constant until 10·33 hr, when outflow began to decline gradually. At 12 hr, outflow increased again from 16 to 20 mm hr^{-1} and remained relatively constant until the end of run 1. Drainage from the core ended at 19 hr, 1 hr after rainfall application ended.

For the clay core, outflow increased rapidly, though less rapidly than for the hillslope core, from 11 mm hr^{-1} at 1 hr to 19 mm hr^{-1} at 3 hr (Figure 4B). After this initial pulse, drainage decreased briefly to 16 mm hr^{-1} at 4 hr, before increasing at 5 hr where it was relatively constant at *c*. 18 mm hr^{-1}. Outflow remained at this rate until 11 hr, when drainage increased and reached a maximum of 20 mm hr^{-1}. Drainage then decreased gradually and remained constant until drainage ended at 20 hr, 2 hr after rainfall application ended.

Run 2. Outflow rate means and ranges for run 2 were similar for the hillslope and clay cores. Hillslope core outflow began 0·17 hr after rainfall application, ranged from 26 to 52 mm hr^{-1}; and averaged 40·5 mm hr^{-1}. Clay core outflow began 0·3 hr after rainfall application, ranged from 25 to 50 mm hr^{-1}; and averaged 39·5 mm hr^{-1}. Outflow from each core was irregular and was marked by two drainage pulses of similar magnitudes (Figure 4C and 4D).

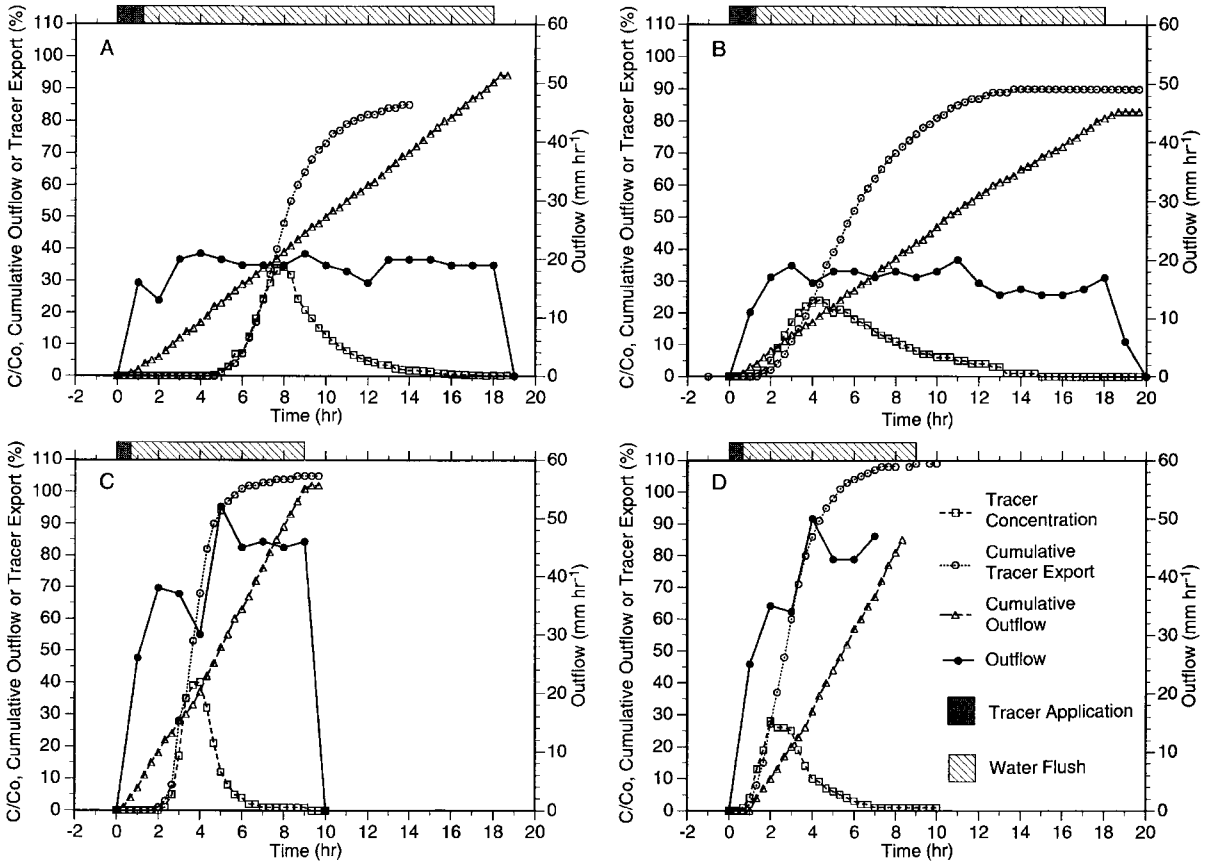

Figure 4. Relative tracer concentration (C/C_o), outflow rate and cumulative tracer export and outflow: (A) Run 1 (Cl^- rainfall application rate of 20 mm hr^{-1}) for the hillslope core; (B) run 1 for the clay core; (C) run 2 (Br^- rainfall application rate of 40 mm hr^{-1}); and (D) run 2 for the clay core

For the hillslope core, outflow increased from 26 mm hr^{-1} at 1 hr to 38 mm hr^{-1} at 2 hr into run 2. Outflow decreased slightly to 37 mm hr^{-1} at 3 hr, before decreasing to 30 mm hr^{-1} at 4 hr. Drainage increased significantly to 52 mm hr^{-1} at 5 hr. By 6 hr, the second drainage pulse had passed through the core and outflow decreased to 45 mm hr^{-1}; where it remained relatively constant until rainfall ended at 9 hr. Drainage from the core ended by 10 hr, 1 hr after rainfall application ended.

For the clay core, outflow increased from 25 mm hr^{-1} at 1 hr to 35 mm hr^{-1} at 2 hr (Figure 4D). Outflow decreased to 34 mm hr^{-1} at 3 hr and increased rapidly to 50 mm hr^{-1} at 4 hr. Outflow at 5 and 6 hr was steady at 44 mm hr^{-1} before increasing to 47 mm hr^{-1} at 7 hr into run 2. Owing to spillage of the outflow collection vials, outflow from 7 to 9 hr was omitted from the graph. Drainage from the core ended at 10 hr, 1 hr after rainfall application ended.

Breakthrough curves

Run 1. The temporal trends in the tracer outflow are presented as the exported relative concentration (C/C_o) of the respective tracer for each 0·33 hr time unit (also see Table II). The Cl^- tracer was first detected in the hillslope core outflow after 4·66 hr (Figure 4A). Outflow relative Cl^- concentration increased gradually between 5 and 6 hr and increased markedly to 0·23 at 7 hr. Outflow Cl^- concentration reached a maximum of 0·35 at 8·2 hr and decreased to 0·05 at 12 hr. A relatively gradual recession occurred from 12 to 18·2 hr, when Cl^- ceased to appear in outflow. Of the applied Cl^- 48% was recovered between 4·66 and

8·2 hr, 32% between 8·2 and 12 hr, and 5% from 12 hr to the end of run 1, making a total of 85% of applied Cl^- recovered. The Cl^- in the outflow was normally distributed from 4·66 to 12 hr; resulting in a unimodal, symmetrical BTC. The Cl^- transport is consistent with the outflow hydrograph because drainage was constant during the same period at *c*. 20 mm hr^{-1}.

For the clay core, the Cl^- tracer first arrived in the outflow 1 hr into run 1 and increased steadily to a BTC peak of 0·24 at approximately 4·66 hr (Figure 4B). Outflow Cl^- concentration decreased at 5 hr and rose slightly at 5·66 hr forming the second BTC maximum. The outflow relative Cl^- concentration decreased gradually for the remainder of run 1. Drainage from the core ended at 15·4 hr, 2·2 hr before rainfall ended. Of the applied Cl^-, 35% was recovered from 1 to 4·66 hr, 9% from 4·66 to 5·33 hr and 46% of applied Cl^- was recovered during the remainder of run 1. The total applied Cl^- recovery was 90%.

Run 2. Bromide was first observed in the hillslope core outflow at 1·66 hr, and reached a maximum relative concentration of 0·40 at 4 hr into run 2 (Figure 4A). Applied Br^- decreased rapidly until 5·33 hr, when Br^- outflow continued to decrease but in a relatively gradual manner. Bromide recovery was 60% from 1·66 to 4 hr. A total of 97% of applied Br^- was recovered at 5·33 hr. Bromide drainage from the core ended at 9·66 hr, 0·66 hr after rainfall application ended.

Bromide export for the clay core began at 0·66 hr and increased to a BTC peak of 0·28, 2 hr into run 2 (Figure 4D). Tracer export decreased to 0·26 until 3 hr, before decreasing gradually throughout the remainder of run 2. Total applied Br^- recovery was 27 and 58%, respectively, by 2 and 3 hr into run 2. Of the total applied Br^-, 51% was recovered throughout the remainder of run 2. Bromide drainage from the core ended at 10 hr, 1 hr after rainfall application ended.

Tensiometer responses

In all experiments, each of the three tensiometers responded simultaneously to applied rainfall and returned to higher tension within 0·17 hr of the end of rainfall (Figure 5). Tensiometer data show that neither core was fully saturated during runs 1 and 2. It is unclear whether minor fluctuations in tension from the top and middle tensiometers are a result of rainfall infiltration, inadvertent variations in the rainfall application rate or wetting front perturbations, as reported elsewhere (Tindall *et al*., 1992). A consecutive, progressive shift in tensiometer response from the core top to bottom was expected to precede drainage of matrix water. However, the simultaneous tensiometer responses in each core during each run and the pulsing of core drainage suggest that preferential pathways influence water movement in each core regardless of rainfall application rate.

Run 1. For the hillslope core, matric potentials for each tensiometer remained relatively constant throughout run 1, following an initial response upon wetting (Figure 5A). This agrees with the relatively constant drainage rate and uniform concentration increase and decrease of Cl^- in core effluent.

For the clay core, the bottom tensiometer matric potential remained constant throughout run 1 (Figure 5B). Tensiometer responses in the top and middle horizons of the clay core correspond with the hydrograph results. Clay core top and middle tensiometers indicated 'wetting-up' from 0 to 2 hr, which is consistent with the first appearance of Cl^- in outflow at 1·33 hr and the initial drainage pulse peak at 3 hr (Figure 4B). The BTC peak at 4·33 hr is consistent with the passage of the initial drainage pulse peak. A second BTC peak occurred at 5·33 hr. Matric potential of the top and middle horizons remained relatively constant, but exhibited a slight trend of increasing matric potential between 3 and 11 hr. During this period, outflow was relatively constant at *c*. 18 mm hr^{-1} and Cl^- concentration in outflow decreased gradually (often referred to as BTC tailing) from 5·33 hr for the remainder of the run. Outflow decreased to *c*. 15 mm hr^{-1} at 15 hr as the mean matric potential of the top and middle tensiometers increased slightly for the remainder of run 1.

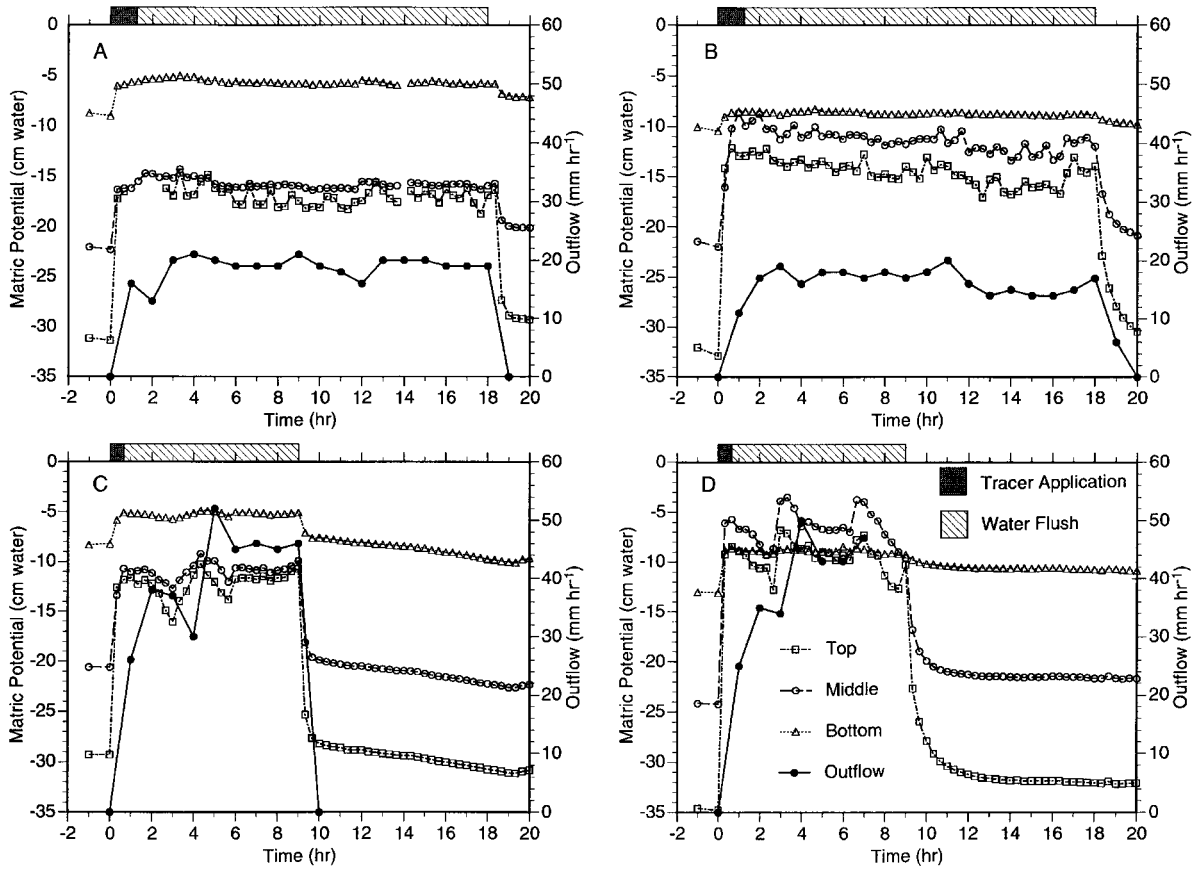

Figure 5. Temporal and spatial variations in soil moisture tension (matric potential) and outflow rate: (A) run 1 (Cl^- rainfall application rate of 20 mm hr^{-1}) for the hillslope core; (B) run 1 for the clay core; (C) run 2 (Br^- rainfall application rate of 40 mm hr^{-1}) for the hillslope core, and; (D) run 2 for the clay core

Run 2. Consistent with all runs, tensiometers responded simultaneously upon the application of rainfall to the hillslope core during run 2. From 0 to 2·33 hr into run 2, the matric potential of the top and middle tensiometers decreased from −30 and −21 to −12 and −11 cm H_2O, respectively, which is consistent with the occurrence of the first drainage pulse (Figure 5C). Matric potential at the top and middle tensiometers increased slightly between 2·33 and 2·66 hr, coinciding with a relative Br^- concentration (C/C_o) increase from 0·01 to 0·17 at 2·33 and 3 hr, respectively. Matric potential then decreased until 4·33 hr, which is consistent with the BTC peak at 4 hr and the second drainage pulse peak at 5 hr. Bromide concentration in drainage decreased rapidly by 6 hr. Both the matric potential of the top and middle horizons and outflow remained relatively constant throughout the remainder of run 2.

For the clay core, tensiometer responses are also consistent with the hydrograph and BTC results from run 2. The matric potential of all tensiometers decreased immediately upon the application of rainfall (Figure 5D). The matric potential of both the top and middle tensiometers then increased until 2 hr, coincident with the first drainage peak at 2 hr and the BTC peak at 2·33 hr. The matric potential of the top and middle horizons increased rapidly from 2·33 to *c*. 3 hr as Br^- concentration in drainage decreased and the second drainage pulse began. Matric potential of the top and middle tensiometers decreased by *c*. 3·33 hr, which is consistent with the second drainage pulse peak of 50 mm hr^{-1} and the rapid movement of the Br^- tracer solution to the core base.

Table III. Mobile water content (θ_m), and dispersivity (ε) values obtained from application of the approximate analytical model of Rose *et al.* (1982) for the hillslope and clay cores during runs 1 and 2. Model efficiencies were derived from a trial and error optimization equation, as presented in Buttle and Leigh (1995)

Core and run	θ_m	ε	Model efficiency
Hillslope core			
Run 1	0·445	0·009	0·95
Run 2	0·430	0·0054	0·99
Clay core			
Run 1	0·300	0·053	0·99
Run 2	0·290	0·035	0·98

Modelling

The approximate analytical model (Rose *et al.*, 1982) efficiencies and Darcian equivalents for mobile water content (θ_m) and dispersivity (ε) for each core during runs 1 and 2 are listed in Table III. Model efficiencies for each run equalled or exceeded 95%.

Run 1. The hillslope core in run 1 had a θ_m of 0·445 — the highest mobile water content for any core or run. Furthermore, ε was 0·009 m, which was relatively small compared with the other core and runs. The small ε, high θ_m and symmetrical BTC indicate a well-drained porosity and limited mixing between the matrix and macrochannels. The clay core θ_m was 0·300 for the same run indicating that water moved through a smaller effective pore geometry than in the hillslope core. However, ε was 0·053, which was relatively high compared with the hillslope core. The relatively high ε, asymmetrical BTC and pulsing of core drainage suggest that water and tracer were partly exchanged between the matrix and macrochannels.

Run 2. The hillslope core θ_m in run 2 was 0·430, only slightly less than that for run 1 (Table III), indicating a large contributing area to flow. However, ε was 0·0054, the lowest of the four experiments, suggesting the most limited exchange of water and tracer between the matrix and macrochannels occurred during this run. For the clay core, θ_m was 0·290, which indicates that the clay core had the smallest effective pore geometry contributing to flow relative to the other rainfall simulations. The clay core ε was 0·035, which suggests a relatively large exchange of water and tracer between matrix and macrochannels.

In summary, the model produced higher θ_m and lower ε values for the hillslope core than the clay core. This is indicative of a higher effective pore geometry and more mixing between pre-event and event water in the hillslope relative to the clay core. Furthermore, tracer appeared later in the outflow from the hillslope than in the clay core for all experiments, indicating a larger contribution of flow from the matrix in the hillslope core.

DISCUSSION

Physical and chemical response of the cores

It should be noted that we do not have any direct evidence pertaining to core soil structures. We have inferred soil structure differences between the hillslope and clay cores. In particular, inferences regarding soil structure are based on previous studies in which clay soils, similar to those collected from the ridge site, have been shown to have macrochannels (Bouma *et al.*, 1977, 1978; Bouma and Dekker, 1978; Jardine *et al.*, 1990). Our inferences also come from direct field observations of cracking and interpedal structure revealed during the core extraction process at PMRW.

Run 1. Matrix flow dominated water and tracer delivery from the hillslope core during run 1. Although initial tensiometer data suggest that macrochannels preferentially channelled event water to depth, concentration gradients may have caused event water within macrochannels to move into the matrix. Matrix flow then appeared to dominate water and tracer delivery in the hillslope core throughout run 1.

Previous studies have shown that when rainfall intensity exceeds the conductivity of matrix pores, water overflows from the matrix into larger, interpedal macrochannels, which then transmit water to depth (van Genuchten and Wierenga, 1976; Bouma and Dekker, 1978; Beven, 1981; Beven and Germann, 1982; Booltink, 1994). At depth, however, some of the tracer in event water moves from macrochannels into the matrix owing to hydraulic and concentration gradients. This corresponds with the results of Jardine *et al*. (1990), who monitored Br^- movement in a soil pedon in the Walker Branch Watershed, Tennessee. Similar water and solute movement has been observed by Luxmoore *et al*. (1990) and Huntington *et al*. (1994). However, in these other studies the soils were drier prior to tracer mobility, and hydraulic gradients probably had a more dominant role in controlling tracer movement into the matrix than for the experiments described here.

For the hillslope core, macrochannel event water appeared to displace pre-event water producing the first drainage pulse of tracer-free water from 0·13 to 2 hr into run 1. Water and tracer then moved to depth through the matrix for the remainder of run 1, as suggested by the relatively large θ_m. The modelled, low ε indicates that water and tracer exchange between the matrix and macrochannels was limited (Smettem, 1984; De Smedt *et al*., 1986; Youngs and Leeds-Harrison, 1990; Buttle and Leigh, 1995) which suggests predominantly matrix flow. In addition, outflow remained relatively constant at *c*. 20 mm hr^{-1} after 3·2 hr. The lack of any distinct large drainage pulses is characteristic of matrix flow. The gradual increase and decrease in tracer concentration is indicative of a well-mixed, constant transport of tracer commonly attributed to matrix flow (Freeze and Cherry, 1979; Nkedi-Kizza *et al*., 1982; Seyfried and Rao, 1987; Youngs and Leeds-Harrison, 1990; Buttle and Leigh, 1995).

For the clay core, both preferential and matrix flow appeared to transport water and tracer during run 1. Preferential flow appeared to displace pre-event water to produce the first drainage pulse of tracer free water from 0·17 to 1·66 hr into run 1 (Figure 4B). Concurrently, we infer that pre-event and event water mixed behind the 'displacement front' before moving to depth through macrochannels. The mixing of pre-event and event water also is supported by the BTC results. Asymmetrical BTCs, marked by a rapid increase to tracer maximum followed by a gradual decrease, and having an early arrival of tracer in the outflow, are commonly attributed to preferential flow. Such BTCs depict tracer by-passing of the tortuous soil matrix as described by the mobile–immobile model (MIM) of van Genuchten and Wierenga (1976). Seyfried and Rao (1987) and Binley *et al*. (1996) obtained similar BTCs, which were attributed to preferential flow. Model results from this experiment (relatively low θ_m and a high ε) indicate that water moved through a smaller effective pore geometry than in the hillslope core, and water and tracer were exchanged between the matrix and macrochannels of the clay core. The asymmetric BTC, initial drainage pulse and model results suggest that water and tracer were preferentially transported in the clay core through a relatively small pore space between 1 and 5·2 hr.

After the passage of the initial drainage pulse between 1 to 5·2 hr, matrix flow appears to have dominated in the clay core. We suggest that tracer was flushed gradually from the matrix after the passage of the initial tracer pulse, as discussed in van Genuchten and Wierenga (1976) and observed by Seyfried and Rao (1987). The extensive BTC tailing between 5·33 and 15 hr substantiates this and is consistent with the results of Seyfried and Rao (1987), who conducted miscible displacement experiments on unsaturated, undisturbed clay loam soil cores and evaluated the BTCs. Seyfried and Rao (1987) concluded that when changing from saturated to unsaturated conditions, water drains from the macrochannels first, which allows air to enter these large pores. Because of the impedance effect of air on water and tracer movement from the matrix into the macrochannels, the hydraulic conductivity of the soil then becomes that of the matrix only, decreasing the effective pore geometry (Seyfried and Rao, 1987). In this experiment, the limited exchange of water and tracer between the matrix and macrochannels may have been caused by air impedance, also described by Youngs and Leeds-Harrison (1990).

Run 2. Water and tracer appeared to be transported by matrix flow in the hillslope core during run 2. It is likely that water and tracer moved very rapidly through the matrix as indicated by the very slight tailing of the Br^- BTC. The modelled θ_m, which was the second highest of all runs, is indicative of matrix flow and therefore supports this conceptual model. The small modelled ε is typical of a small exchange between macrochannels and the soil matrix. The tensiometer data, limited BTC tailing and large θ_m suggest that the high intensity rainfall flushed event water and tracer through the soil matrix quickly.

For the clay core during run 2, preferential and matrix flow appear to have contributed to vertical water and tracer transport. Rainfall intensity exceeded matrix infiltration capacity (McDonnell, 1990) which may have resulted in the overflow of mixed water from the matrix into macrochannels, where mixed water moved to depth. Synchronous tensiometer responses regardless of depth 0·13 hr into run 2 demonstrate this. Also, the appearance of tracer in the outflow at 0·66 hr indicates that event water was transmitted rapidly through the core.

We infer that after the initial tensiometer response, the soil matrix transported water to depth. We hypothesize that, at depth, the matrix 'wetted-up' and transported water into macrochannels, which caused matric potentials to increase in the top of the core from 0 to 2·33 hr. Well-developed interpedal macrochannels that are common in structured clays (Bouma and Dekker, 1978; Bouma *et al*., 1978; Bouma, 1980) and probably are the effective conduits within the core facilitated the rapid tracer movement to depth. The passage of the initial drainage pulse at 3 hr and the 58% Br^- recovery support this conceptual model. As the tracer-free rainfall application continued, event water moved through the matrix, flushing residual tracer from the matrix throughout the remainder of run 2. Slight BTC tailing from 4 to 9 hr corroborates this. The model results indicate that water and tracer were transported through the smallest effective pore geometry relative to all other runs.

Links to ongoing field studies

The results of this laboratory study are corroborated with those of a concurrent hydrometric and hydrochemical field study, conducted from May 1994 to April 1995, at the base of a south-facing hillslope at PMRW (Ratcliffe *et al*., 1996; Peters and Ratcliffe, 1998). The soils at this site were not extensively characterized, but because of similar bedrock geology and landscape position are probably similar to the hillslope soil used here. An evaluation of the timing and flow rate of zero-tension lysimeters and temperature changes of soil and groundwater indicates that rain water was transported rapidly to the saturated zone during moderate (0·1–0·5 mm hr^{-1}) to high ($>0{\cdot}5$ mm hr^{-1}) intensity and high magnitude (>20 mm) rainstorms (Ratcliffe *et al*., 1996). An evaluation of Cl^- concentrations of sequential samples of precipitation, throughfall, soil water and groundwater for the same site also indicate rapid transport of event water to the saturated zone (Peters and Ratcliffe, 1998). Furthermore, mixing between pre-event water in the matrix and event water transported in macropores was not important during the very dry antecedent conditions that typically occur during the growing season, but was important during the dormant season when the catchment was wetter.

The field results are consistent with patterns observed for the degree of mixing and importance of matrix flow in the soil cores of the laboratory study. In both the growing or dormant season, flow from zero-tension lysimeters at depth was rapid (Ratcliffe *et al*., 1996; Peters and Ratcliffe, 1998). Antecedent moisture conditions for soil cores at the onset of the experiments reported herein were most similar to those of the dormant season rainstorms at PMRW (Peters and Ratcliffe, 1998). The relatively large contribution of pre-event water to flow in the zero-tension lysimeters may reflect mixing of matrix and macrochannel water during transport, consistent with the results for the hillslope cores.

CONCLUSIONS

Tracer magnitude and arrival in outflow of large (30 cm diameter by 38 cm long), undisturbed hillslope and ridge (clay) soil cores from the Panola Mountain Research Watershed, Georgia, are affected by soil structure

and rainfall intensity. Soil structure affects the hydrological pathways by which water and tracer are transported through the cores. Two rainfall intensities, 20 and 40 mm hr^{-1}, for separate Cl^- and Br^- amended solutions were applied to the cores. For both the relatively low and high rainfall intensity experiments, preferential flow occurred in the clay soil, but not in the hillslope soil. The preferential flow is attributed to inferred, well-developed interpedal macrochannels, that are commonly found in structured clay soils, and that influence tracer magnitude and time of peak breakthrough.

The existence of macrochannels does not necessarily result in preferential flow along macrochannels to depth in unsaturated soils. Air pockets within macrochannels in unsaturated conditions may impede the movement and mixing of water and tracer between the matrix and macrochannels, confining flow within the soil matrix. Because the matrix fills before the macropores, the matrix may saturate if rainfall intensity is greater than the matrix infiltration capacity. In addition, tree roots as large as 6·4 cm were observed in both the hillslope and clay core. The tree roots may have influenced or discouraged vertical water movement depending on the tree root geometry.

During all experiments, preferential flow occurred to some extent in both soils, independent of soil structure. Consequently, rainfall intensity and inferred soil structure affect the development of subsurface saturation. In this study, each rainfall intensity exceeded the matrix infiltration capacity throughout the clay core, but only at the top of the hillslope core. Nevertheless, evidence of preferential flow was demonstrated by the tensiometer response (hillslope and clay), outflow rate and breakthrough curves for the clay core during each rainfall intensity.

Preferential flow through macrochannels continues as long as the flow rate in them exceeds the rate of absorption into the surrounding matrix. The absorption rate is assumed to be a function of hydraulic and concentration gradients. The exchange of water and tracer between the matrix and macrochannels which, in turn, affect tracer recovery and mass balance, appear to be a function of both the inferred soil structure and rainfall intensity.

ACKNOWLEDGEMENTS

This study was conducted in cooperation with the Georgia Department of Natural Resources. The work was funded through the National Science Foundation (Grant EAR 9406436). We are grateful to: K. Beven, J. Freer, K. Kim, H. Green and A. Zumbuhl for assistance in the field; D. Radcliffe (UGA) and J. Dowd for valuable insight into the experimental design; D. Brammer for assistance in conducting the laboratory experiments; J. Buttle for valuable discussions; and J. Shanley and T. Huntington for constructive comments on an earlier draft of the manuscript. We are also grateful to the staff of the Panola Mountain State Conservation Park, which provided access to the site and other ancillary support.

REFERENCES

Anderson, J. L. and Bouma, J. 1977. 'Water movement through pedal soils II. Unsaturated flow', *Soil Sci. Soc. Am. J.*, **41**, 419–423.
Beven, K. J. 1981. 'Micro-, meso-, macroporosity and channeling flow phenomena in soils', *Soil Sci. Soc. Am. J.*, **45**, 1245.
Beven, K. J. and Germann, P. 1982. 'Macropores and water flow in soils', *Wat. Resour. Res.*, **18**, 1311–1325.
Binley, A., Henry-Poulter, S., and Shaw, B. 1996. 'Examination of solute transport in an undisturbed soil column using electrical resistance tomography', *Wat. Resour. Res.*, **32**, 763–769.
Booltink, H. W. G. 1994. 'Field-scale distributed modeling of bypass flow in a heavy textured clay coil', *J. Hydrol.*, **163**, 65–84.
Bouma, J. 1980. 'Field measurement of soil hydraulic properties characterizing water movement through swelling clay coils', *J. Hydrol.*, **45**, 149–158.
Bouma, J. 1981. 'Comment on ''Micro-, meso-, and macroporosity of soil'' ', *Soil Sci. Soc. Am. J.*, **45**, 1244–1245.
Bouma, M. and Dekker, L. W. 1978. 'A case study on infiltration into dry clay soil. I. Morphological observations', *Geoderma*, **20**, 27–40.
Bouma, J., Jongerius, A., Boersma, O., Jager, A., and Schoonderbeek, D. 1977. 'The function of different types of macropores during saturated flow through four swelling soil horizons', *Soil Sci. Soc. Am. J.*, **41**, 945–950.
Bouma, M., Dekker, L. W., and Wosten, J. H. M. 1978. 'A case study on infiltration into dry clay soil II. Physical measurements', *Geoderma*, **20**, 41–51.

Buttle, J. M. and Leigh, D. G. 1995. 'Isotopic and chemical tracing of macropore flow in laboratory columns under simulated snowmelt conditions', *IAHS Publ.*, **229**, 67–76.
Cappellato, R. and Peters, N. E. 1995. 'Dry deposition and canopy leaching rates in deciduous and coniferous forests of the Georgia Piedmont: an assessment of a regression model', *J. Hydrol.*, **169**, 131–150.
Chen, C. and Wagenet, R. J. 1992. 'Simulation of water and chemicals in macropore soils: Part I. Representation of the equivalent macropore influence and its effect on soilwater flow', *J. Hydrol.*, **130**, 105–126.
Chichester, F. W. and Smith, S. J. 1978. 'Disposition of ^{15}N-labelled fertilizer nitrate applied during corn culture in field lysimeters', *J. Environ. Qual.*, **7**, 227–233.
De Smedt, F., Wauters, F., and Sevilla, J. 1986. 'Study of tracer movement through unsaturated sand', *J. Hydrol.*, **85**, 169–181.
Freer, J., McDonnell, J., Beven, K. J., Brammer, D., Burns, D. A., Hooper, R. P., and Kendall, C. 1997. 'Topographic controls on subsurface storm flow at the hillslope-scale for two hydrologically distinct small catchment', *Hydrol. Proc.*, **11**, 1347–1352.
Freeze, R. A. and Cherry, J. A. 1979. *Groundwater*. Prentice Hall, Englewood Cliffs, New Jersey. 604 pp.
Huntington, T. G., Hooper, R. P., Peters, N. E., Bullen, T. D., and Kendall, C. 1993. *USGS Open File Report 93-55*, *Water Energy, and Biogeochemical Budgets Investigation at Panola Mountain Research Watershed, Stockbridge, Georgia–A Research Plan*. USGS., Atlanta, Georgia.
Huntington, T. G., Blum, A. E., and White, A. F. 1994. 'Migration of a bromide tracer in a forest soil in the Georgia Piedmont', *EOS, Trans. Am. Geophys. Union*, **75**, 150 (abstract).
Jabro, J. D., Lotse, E. G., Fritton, D. D., and Baker, D. E. 1994. 'Estimation of preferential movement of bromide tracer under field conditions', *J. Hydrol.*, **156**, 61–71.
Jardine, P. M., Wilson, G., and Luxmoore, R. J. 1990. 'Unsaturated solute transport through a forest soil during rain storm events', *Geoderma*, **46**, 103–118.
Klute, A. and Dirksen, C. 1986. 'Hydraulic conductivity and diffusivity: laboratory methods', in: Klute, A. (ed.), *Methods of Soil Analysis, Physical and Mineralogical Methods*, Part 1, no. 9, 2nd edn. American Society of Agronomy, Inc. and Soil Science Society of America, Inc., Madison. pp. 687–734.
Kung, K.-J. S. 1990. 'Preferential flow in a sandy vadose zone: 1. Field observation', *Geoderma*, **46**, 51–71.
Luxmoore, R. J. 1981. 'Micro-, meso-, and macroporosity of soil', *Soil Sci. Soc. Am. J.*, **45**, 671–672.
Luxmoore, R. J., Jardine, P. M., Wilson, G. V., Jones, J. R., and Zela, L. W. 1990. 'Physical and chemical controls of preferred flow through a forested hillslope', *Geoderma*, **46**, 139–154.
McDonnell, J. J. 1990. 'A rationale for old water discharge through macropores in a steep, humid catchment', *Wat. Resour. Res.*, **26**, 2821–2832.
McDonnell, J. J. 1993. 'Electronic versus fluid multiplexing in recording tensiometer systems', *Am. Soc. Agric. Eng.*, **36**, 459–462.
McDonnell, J. J., Freer, J., Hooper, R., Kendall, C., Burns, D., Beven, K., and Peters, J. 1996. 'New method developed for studying flow on hillslopes', *EOS Trans. Am. Geophys. Union*, **77**, 465–472.
Mosley, M. P. 1979. 'Streamflow generation in a forested watershed, New Zealand', *Wat. Resour. Res.*, **15**, 795–806.
Nkedi-Kizza, P., Rao, P. S. C., Jessup, R. E., and Davidson, J. M. 1982. 'Ion exchange and diffusive mass transfer during miscible displacement through an aggregated oxisol', *Soil Sci. Soc. Am. J.*, **46**, 471–476.
Peters, N. E. 1994. 'Water-quality variations in a forested Piedmont catchment, Georgia, USA', *J. Hydrol.*, **156**, 73–90.
Peters, N. E. and Ratcliffe, E. B. 1998. 'Tracing hydrologic pathways using chloride at the Panola Mountain Research Watershed, Georgia, USA', *Wat. Air Soil Pollut.*, **105**, 263–275.
Rao, P. S. C., Rolston, D. E., Jessup, R. E., and Davidson, J. M. 1980a. 'Solute transport in aggregated porous media: theoretical and experimental evaluation', *Soil Sci. Soc. Am. J.*, **44**, 1139–1146.
Rao, P. S. C., Jessup, R. E., Rolston, D. E., Davidson, J. M., and Kilcrease, D. P. 1980b. 'Experimental. and mathematical description of nonadsorbed solute transfer by diffusion in spherical aggregates', *Soil Sci. Soc. Am. J.*, **44**, 684–688.
Ratcliffe, E. B., Peters, N. E., and Tranter, M. 1996. 'Short-term hydrological response of soil water and groundwater to rainstorms in a deciduous forest hillslope, Georgia, USA', in Anderson, M. G. and Brooks, S. M. (eds), *Advances in Hillslope Processes*, Vol. 1. Wiley, London. pp. 129–147.
Rose, C. W., Chichester, W., Williams, J. R., and Ritchie, J. T. 1982. 'Application of an approximate analytical method of computing solute profiles with dispersion in soils', *J. Environ. Qual.*, **11**, 151–155.
Sami, K. and Buttle, J. M. 1991. 'Comparison of measured and estimated unsaturated hydraulic conductivities during snowmelt recharge processes during snowmelt: an isotopic and hydrometric investigation. *J. Hydrol.*, **123**, 243–259.
Seyfried, M. S. and Rao, P. S. C. 1987. 'Solute transport in undisturbed columns of an aggregated tropical soil: preferential flow effects', *Soil Sci. Soc. Am. J.*, **51**, 1434–1444.
Skopp, J., Gardner, W. R., and Tyler, E. J. 1981. 'Solute movement in structured soils: two region model with small interaction', *Soil Sci. Soc. Am. J.*, **45**, 837–842.
Smettem, K. R. J. 1984. 'Soil-water residence time and solute uptake 3. Mass transfer under simulated winter rainfall conditions in undisturbed soil cores. *J Hydrol.*, **67**, 235–248.
Smettem, K. R. J. 1986. 'Analysis of water flow from cylindrical macropores', *Soil Sci. Soc. Am. J.*, **50**, 1139–1142.
Tindall, J. A., Hemmen, K., and Dowd, J. F. 1992. 'An improved method for field extraction and laboratory analysis of large, intact soil cores', *J. Environ. Qual.*, **2**, 259–263.
Tindall, J. A., Petrusak, R. L., and McMahon, P. B. 1995. 'Nitrate transport and transformation processes in unsaturated porous media', *J. Hydrol.*, **169**, 51–94.
Trudgill, S. T., Pickles, A. M., Smettem, K. R. J., and Crabtree, R. W. 1983. 'Soil water residence time and solute uptake 1. Dye tracing rainfall events', *J Hydrol.*, **60**, 257–279.
Tsuboyama, Y., Sidle, R., Noguchi, S., and Hosoda, I. 1994. 'Flow and solute transport through the soil matrix and macropores of a hillslope segment', *Wat. Resour. Res.*, **30**, 879–890.

Tsukamoto, Y. and Ohta, Y. 1988. 'Runoff process on a steep forested slope', *J. Hydrol.*, **102**, 165–178.
van Genuchten, M. Th. and Wierenga, P. J. 1976. 'Mass transfer studies in sorbing porous media 1. Analytical solutions', *Soil Sci. Soc. Am. J.*, **40**, 473–479.
van Stiphout, T. P. J., van Lanen, H. A. J., Boersma, O. H., and Bouma, J. 1987. 'The effect of bypass flow and internal catchment of rain on the water regime in a clay loam grassland soil', *J. Hydrol.*, **95**, 1–11.
Youngs, E. G. and Leeds-Harrison, P. B. 1990. 'Aspects of transport processes in aggregated soils', *J. Soil Sci.*, **41**, 665–675.

